

LAB ROTATION 02

2nd Week Assignment

Seyma Bayrak, Advisor: Philipp Hövel

18.09.2013

1 Nonlinear Dynamics of Neural Networks

1.1 Simple FitzHugh-Nagumo Model

This section is a continuing part of *1st Week Assignment*, it aims to analyze the effect of parameters ε and γ in the equations (1) and (2) given below and to plot trajectories on nullcline graphs.

$$\varepsilon \dot{x} = x - \frac{x^3}{3} - y \quad (1)$$

$$\dot{y} = x + a \quad (2)$$

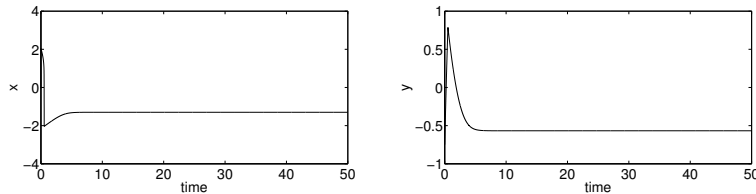


Figure 1, $a = 1.30$, $\varepsilon = 0.005$, $(x_0, y_0) = (-0.05, -0.75)$

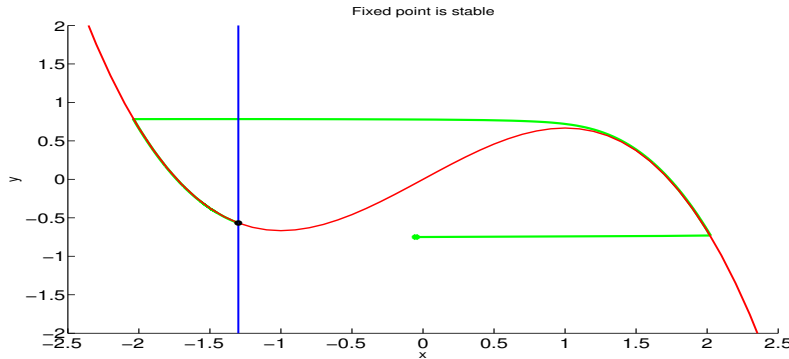


Figure 2, $a = 1.30$, $\varepsilon = 0.005$, $(x_0, y_0) = (-0.05, -0.75)$

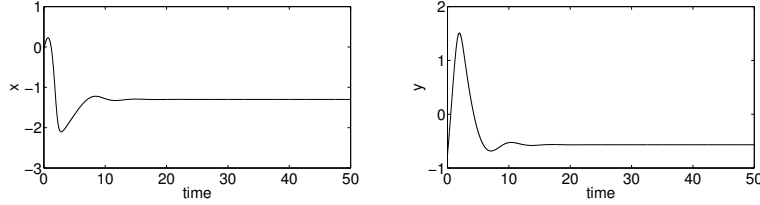


Figure 3, $a = 1.30, \varepsilon = 1, (x_0, y_0) = (-0.05, -0.75)$

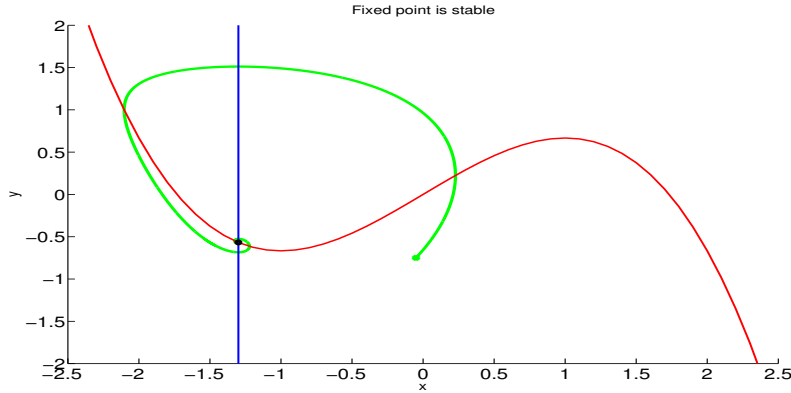


Figure 4, $a = 1.30, \varepsilon = 1, (x_0, y_0) = (-0.05, -0.75)$

- a effect: Bifurcation analysis done in 1st Week Assignment showed that, as long as $|a| > 1$, the system is expected to be stable. Figures 1-4 have $a = 1.30$ and they are all stable, or in other words "excitable".
- ε effect: it does not affect stability but plays a role in the time evolution and pathway of initial points x_0 and y_0 - how long it takes initial point to reach to the stable point. When ε is small, x and y reaches stability faster. In other words, ε brings a separation to the time scales of x and y . The time evolution of x is effected more with ε as equation (1) states, figure 4 shows that x change over time becomes faster with bigger ε when compared with figure 2.

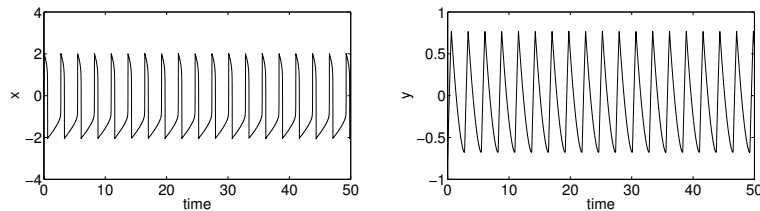


Figure 5, $a = 0.90, \varepsilon = 0.005, (x_0, y_0) = (-0.05, -0.75)$

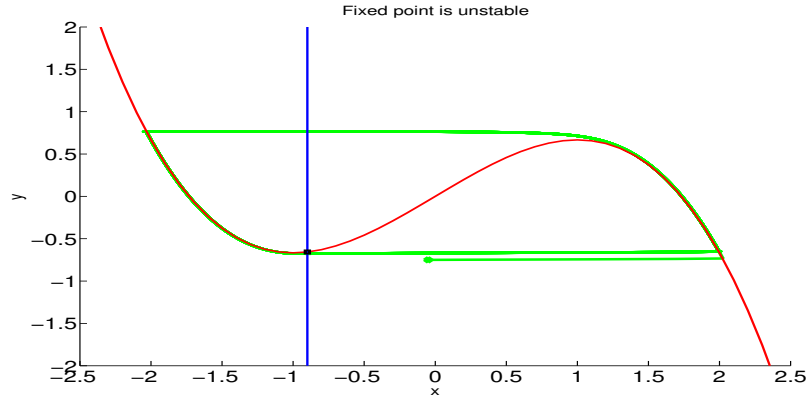


Figure 6, $a = 0.90$, $\varepsilon = 0.005$, $(x_0, y_0) = (-0.05, -0.75)$

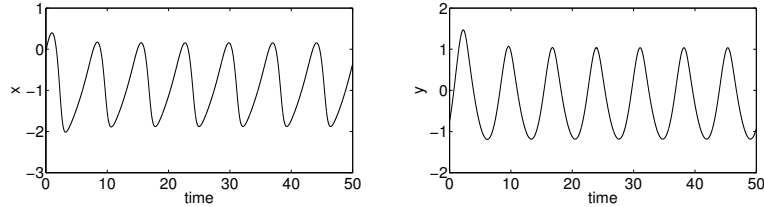


Figure 7, $a = 0.90$, $\varepsilon = 1$, $(x_0, y_0) = (-0.05, -0.75)$

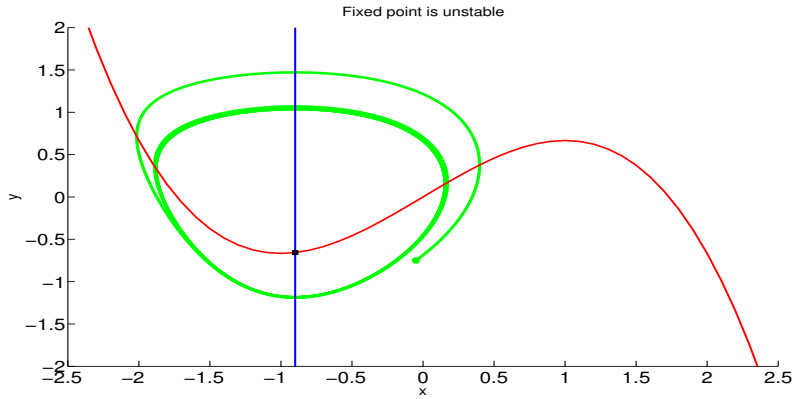


Figure 8, $a = 0.90$, $\varepsilon = 1$, $(x_0, y_0) = (-0.05, -0.75)$

- a effect: When $|a| < 1$, the system is unstable. Figures 5 and 7 have oscillations with $a = 0.90$.
- ε effect: It affects the period of oscillations, when ε is small, oscillatory behavior of x and y happens more frequently, and x evolves slower over time in comparison to y (figure 6 and 8 compared)

1.2 Extended FitzHugh-Nagumo Model

$$\varepsilon \dot{x} = x - \frac{x^3}{3} - y \quad (3)$$

$$\dot{y} = x + a - \gamma y \quad (4)$$

Fixed point can be now *stable*, *unstable*, *saddle*.

Saddle point means that the signs of real parts of the eigenvalues of Jacobian matrix are different. We would like to eliminate saddle points, since saddle point is also unstable.

$$\mathbf{J} = \begin{pmatrix} 1 - x_f^2 & -1 \\ \varepsilon & -\varepsilon\gamma \end{pmatrix}$$

$$\lambda_{1,2} = \frac{trJ \pm \sqrt{tr^2 J - 4\det J}}{2} = \frac{trJ \pm trJ \left(\sqrt{1 - \frac{4\det J}{tr^2 J}} \right)}{2}$$

In order to keep the real part of eigenvalue to be dominated by the first term of the equation above (trJ), the term in square root must be either positive and smaller than 1 or it must be negative, which contributes to λ only with a complex part. This is done by assuming $\det(J) > 0$. Then the sign of the eigenvalues is controlled directly by trJ , it is either positive for λ_1 and λ_2 or negative.

$$\det(J) = \varepsilon(\gamma(x_f^2 - 1) + 1) > 0 \implies 0 < \gamma < 1$$

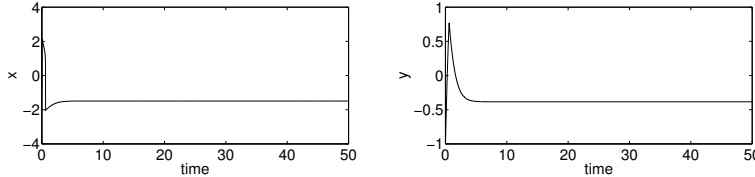


Figure 9, $a = 1.30$, $\varepsilon = 0.005$, $\gamma = 0.5$, $(x_0, y_0) = (-0.75, -1)$

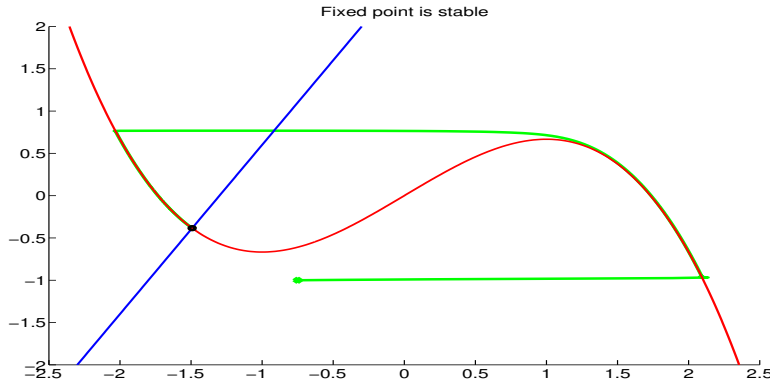


Figure 10, $a = 1.30$, $\varepsilon = 0.005$, $\gamma = 0.5$, $(x_0, y_0) = (-0.75, -1)$

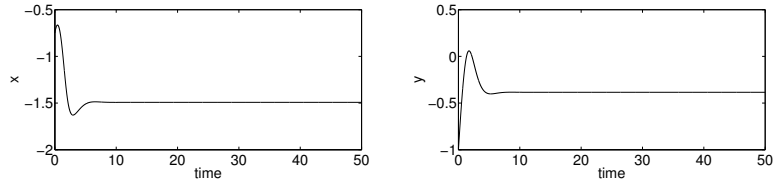


Figure 11, $a = 1.30, \varepsilon = 1, \gamma = 0.5, (x_0, y_0) = (-0.75, -1)$

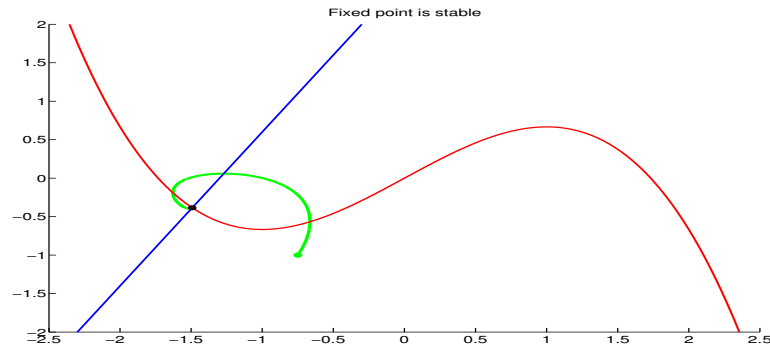


Figure 12, $a = 1.30, \varepsilon = 0.005, \gamma = 0.5, (x_0, y_0) = (-0.75, -1)$

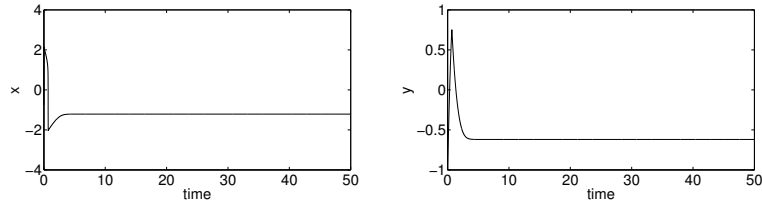


Figure 13, $a = 0.90, \varepsilon = 0.005, \gamma = 0.5, (x_0, y_0) = (-0.75, -1)$

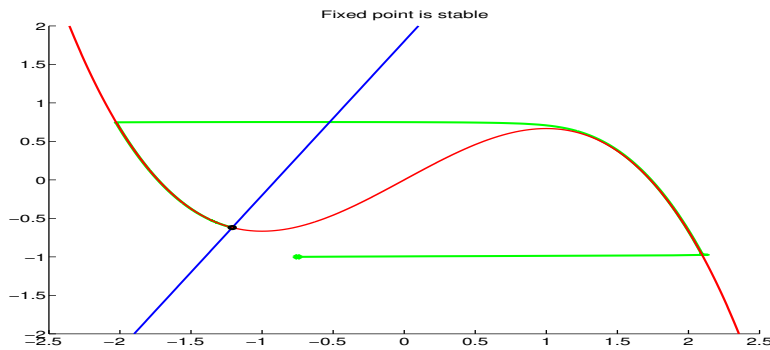


Figure 14, $a = 0.90, \varepsilon = 0.005, \gamma = 0.5, (x_0, y_0) = (-0.75, -1)$

- a effect: When $|a| < 1$, the system was unstable in simple FHN model, however the stability in extended FHN model is now controlled by not only a but also γ . Figures 13 and 14 shows stability with $|a| < 1$ and $\gamma = 0.5$ in opposite to the Figures 5-8.
- ε effect: It affects again the time period of initial points to reach to the stability and pathway of trajectory. Smaller ε brings stability faster in Figure 13 compared to Figure 11.

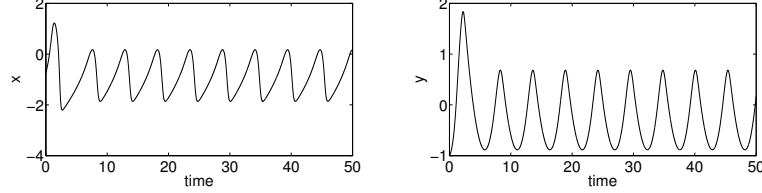


Figure 15, $a = 0.90$, $\varepsilon = 0.4$, $\gamma = 0.05$, $(x_0, y_0) = (-0.75, -1)$

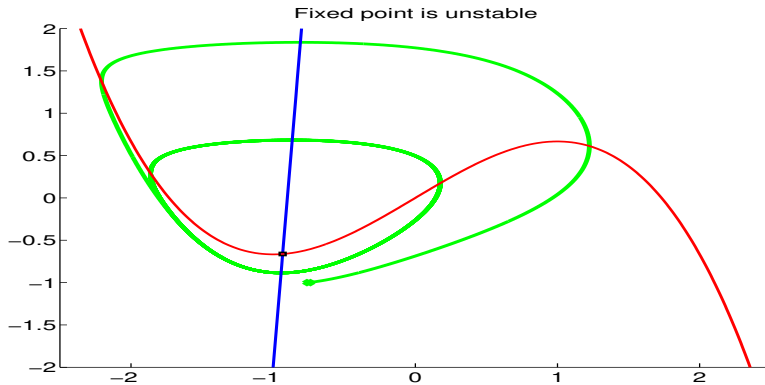


Figure 16, $a = 0.90$, $\varepsilon = 0.04$, $\gamma = 0.05$, $(x_0, y_0) = (-0.75, -1)$

- γ effect: This parameter controls the stability or instability of the system. We already assumed γ between 0 and 1 as it was discussed in bifurcation analysis of extended FHN model. When γ is close to 0, then the system acts unstable and x - y seem to oscillate. Figure 13 ($\gamma = 0.5$) turns into a series of oscillatory behavior for x and y in Figure 15 ($\gamma = 0.05$). Here I did not necessarily keep ε at the same values, but we are already sure that ε has no effect on stability.

2 Isolated FitzHugh-Nagumo Neural Model

[VUK13] paper simulates the neural network dynamics of one node with u_i (attractor) and v_i (inhibitor) by using FHN model as in the following equations;

$$\dot{u}_i = g(u_i, v_i) - c \sum_{j=1}^N f_{ij} u_j(t - \Delta t_{ij}) + n_u \quad (5)$$

$$\dot{v}_i = h(u_i, v_i) + n_v \quad (6)$$

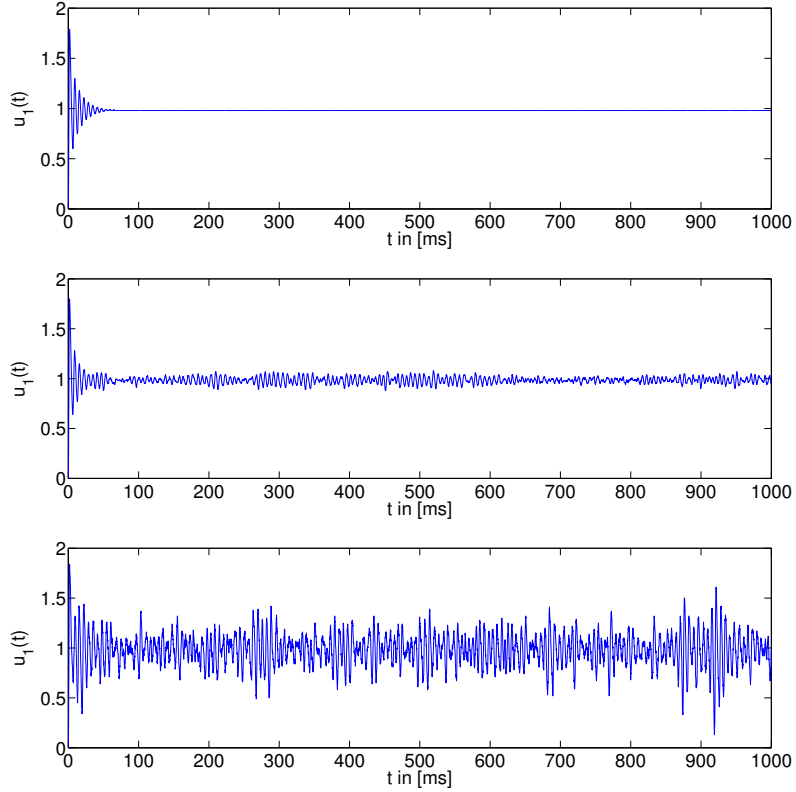
where c is coupling strength, f_{ij} is the connectivity matrix, Δt_{ij} is time delay due to finite signal propagation velocity between nodes, n_u is the noise factor. Δt_{ij} is calculated as $\Delta t_{ij} = \frac{d_{ij}}{\nu}$, distance matrix divided by velocity and noise factor is includes the noise strength D . Note that $i, j = 0, 1, 2, \dots, N$

The functions g and v are modeled very similar to FitzHugh-Nagumo model introduced before:

$$\dot{u} = g(u, v) = \tau(v + \gamma u - \frac{u^3}{3}) \quad (7)$$

$$\dot{v} = h(u, v) = -\frac{1}{\tau}(u - \alpha + bv - I) \quad (8)$$

This section aims to observe the noise strength D on an isolated system meaning no coupling (simply by $c = 0$). Figures below indicate the attractor behavior of the first node u_1 over time with different noise strengths.



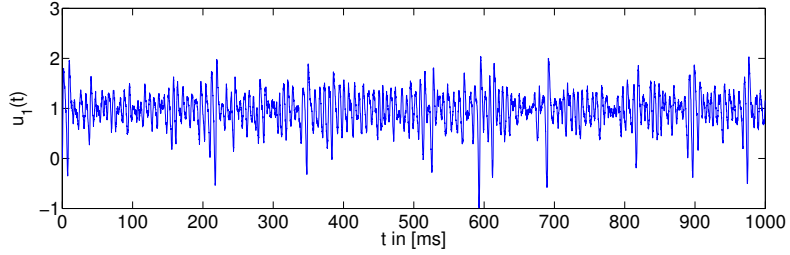
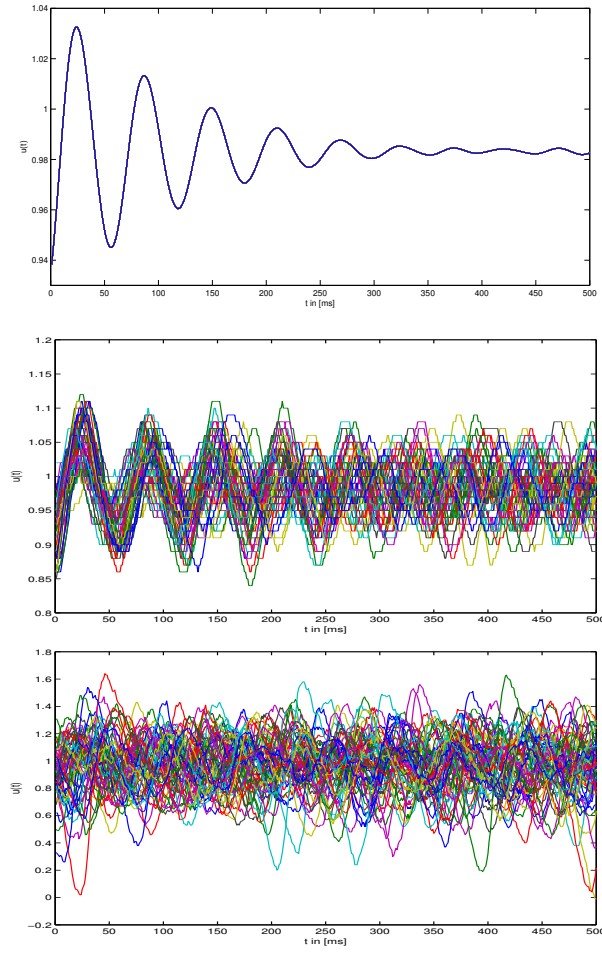


Figure 17, Time evolution of u_1 when $c = 0$, the noise strengths from top to below: $D = 0$, $D = 0.01$, $D = 0.05$, $D = 0.1$ ($I = 0$, $v = 7m/s$, $b = 0.2$, $\tau = 1.25$, $\alpha = 0.85$, $\gamma = 1$, $r = 0.5$)

Now, let us have a look at the attractor behavior of all the isolated nodes $u_i(t)$, $i = 1, 2, 3, \dots, N$ in $t = 500ms$ with different noise strengths.



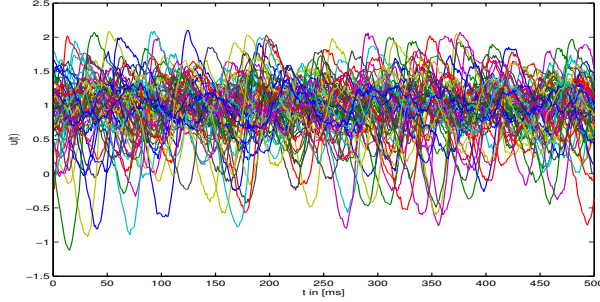


Figure 18, Time evolution of $u_i(t)$ when $c = 0$, the noise strengths from top to below: $D = 0$, $D = 0.01$, $D = 0.05$, $D = 0.1$. ($I = 0$, $v = 7\text{m/s}$, $b = 0.2$, $\tau = 1.25$, $\alpha = 0.85$, $\gamma = 1$, $r = 0.5$) Note that, when the noise strength D is 0, then modelled attractor neuronal activity is same for all $N = 64$ nodes as seen in top of the figure.

3 Distance Distribution between Cortical Regions

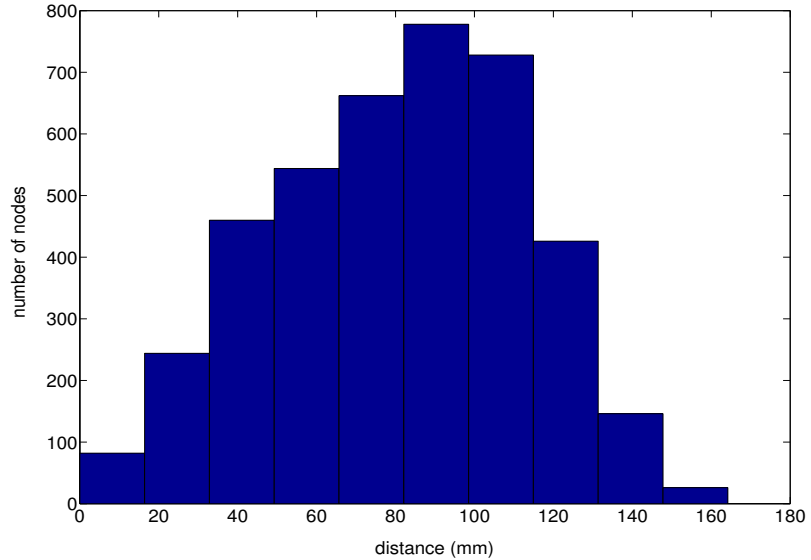


Figure 19, Distance distribution between the $N = 64$ nodes, source: $d_{ij} = FSL_ROIs_distance_matrix.dat$, the distances between nodes are Euclidean.

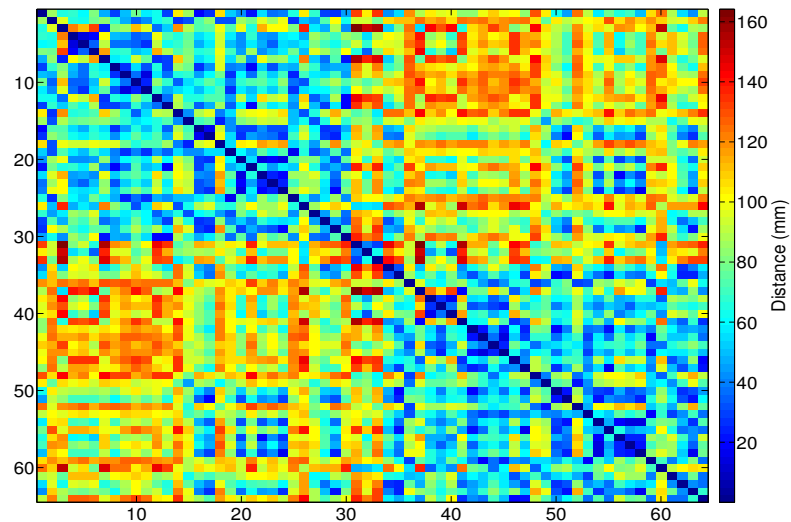


Figure 20, Euclidean distance matrix d_{ij} in color code

4 Correlation Distribution of fMRI Data

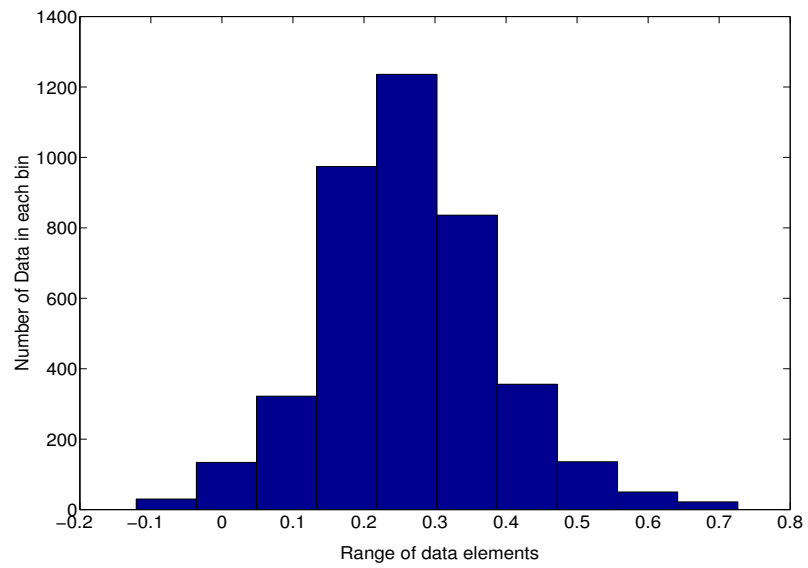


Figure 21, Data distribution in functional connectivity matrix as a result of fMRI signaling,
 $n_{ij}=A.txt$, where $i, j = 1, 2, \dots, N = 64$

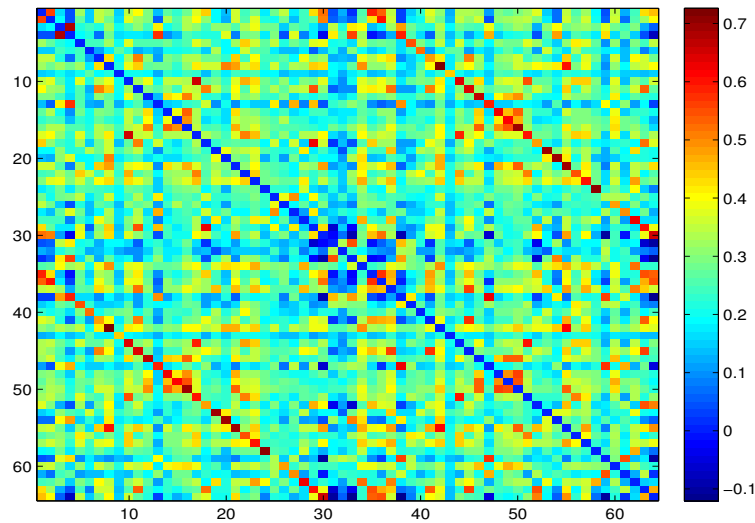


Figure 22, Functional connectivity matrix n_{ij} in color code. $n_{ij}=A.txt$, the correlations among the nodes are not always positive, negative correlations might correspond to the inhibitory effects of nodes on each other.

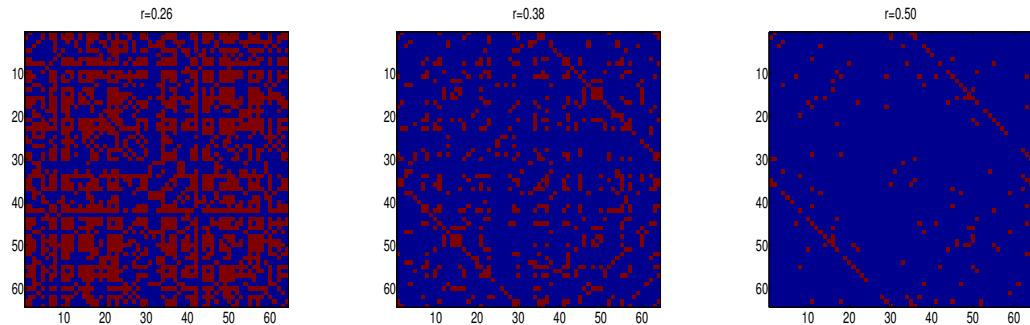


Figure 23, Functional connectivity matrices f_{ij} with applied thresholds in color code, red color for the ones, and blue for the zeros. Figure on the left: $f_{ij}=A_r.0.26.dat$, in the middle: $f_{ij}=A_r.0.38.dat$, on the right: $f_{ij}=A_r.0.50.dat$

5 Visualization of f_{ij} in 2D Anatomical Space with different rs

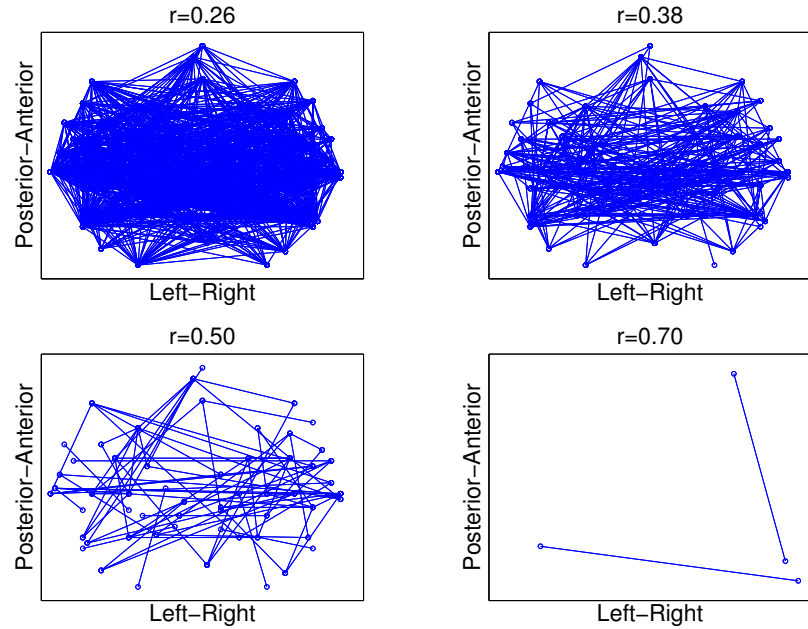


Figure 24, Visualization of threshold matrices in anatomical space by locating each region according to its x and y coordinates and drawing a link between significantly connected regions.

6 Visualization of f_{ij} in 3D Anatomical Space with different r_s

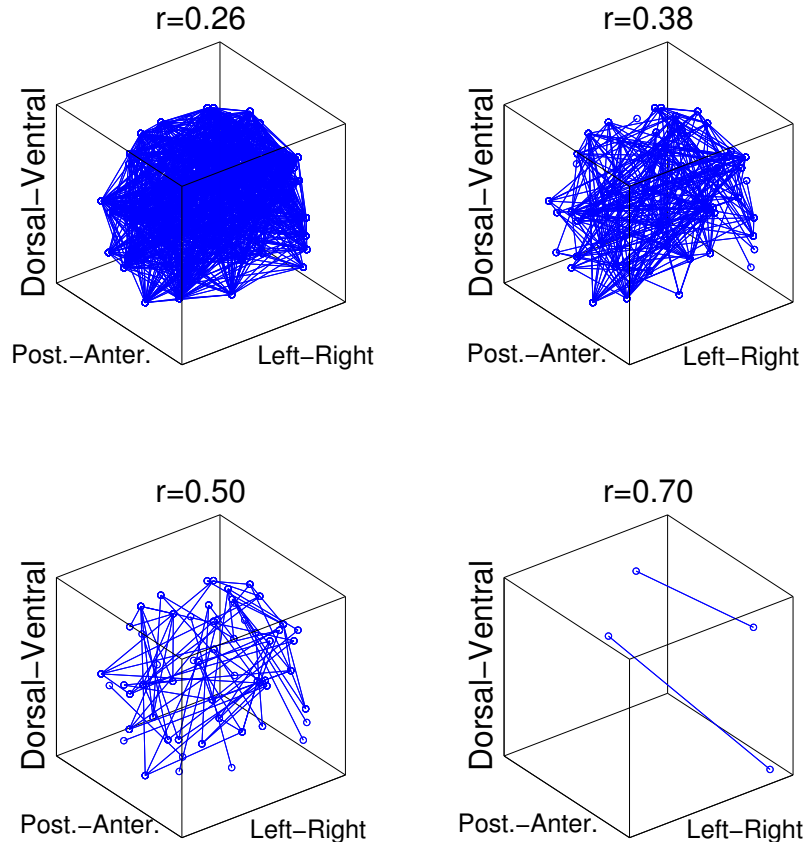


Figure 25, Visualization of threshold matrices in anatomical space by locating each region according to its x , y and z coordinates and drawing a link between significantly connected regions.

7 Simulated Bold Signals with Balloon-Windkessel Model

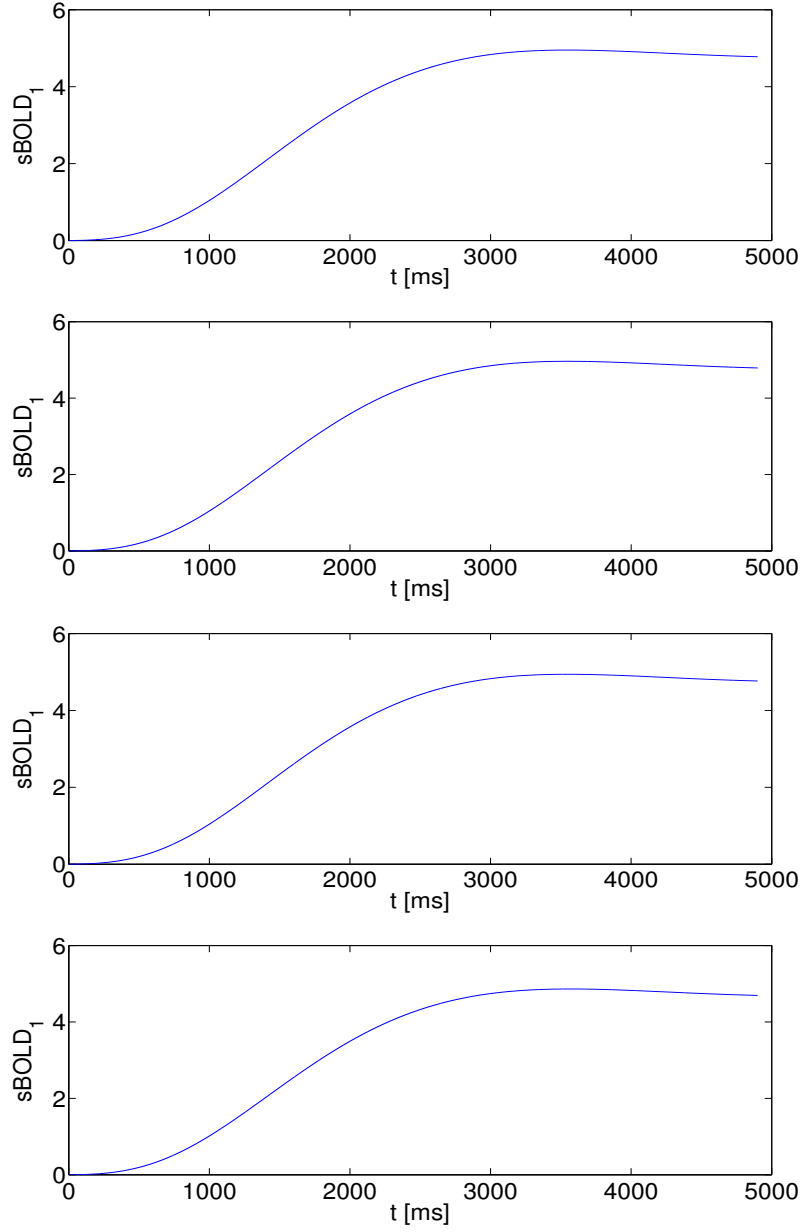


Figure 26, Time evolution of simulated u_1 when $c = 0$, the noise strengths from top to bottom: $D = 0, D = 0.01, D = 0.05, D = 0.1$ ($I = 0, v = 7m/s, b = 0.2, \tau = 1.25, \alpha = 0.85, \gamma = 1, r = 0.5$)

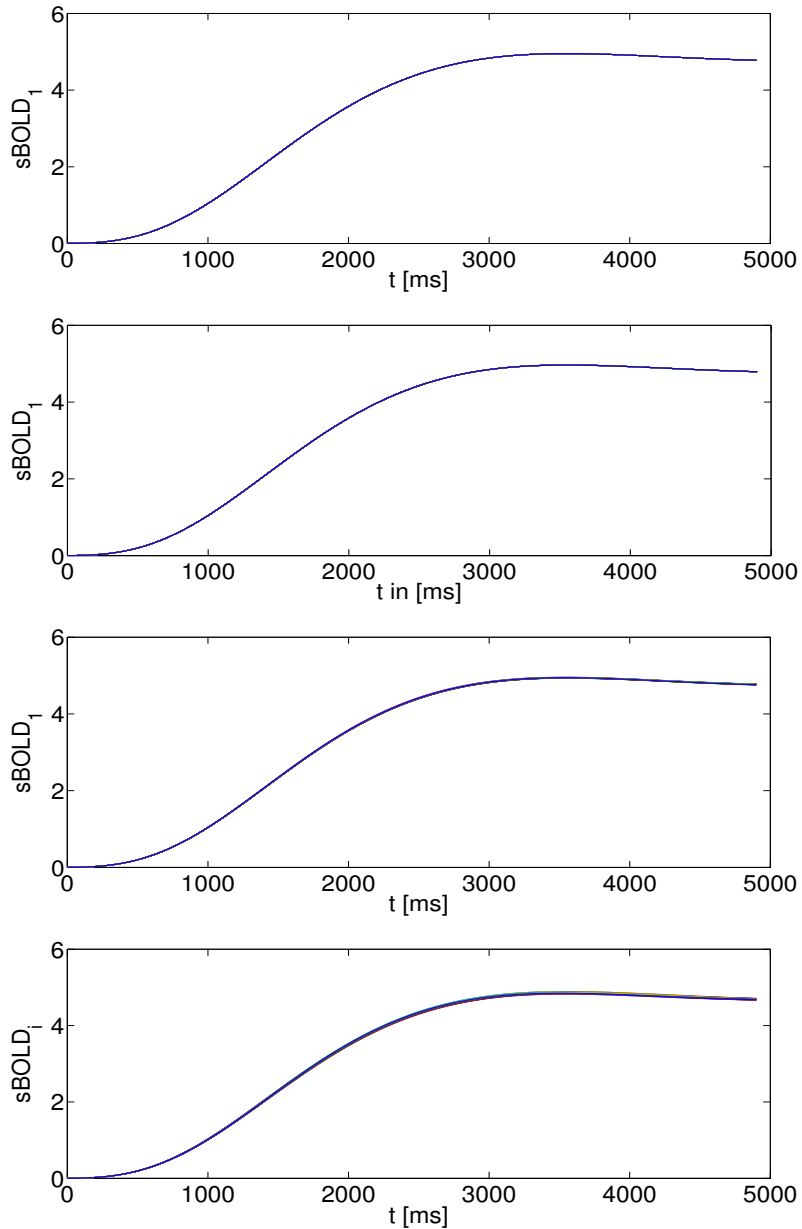


Figure 27, Time evolution of simulated u_i when $c = 0$, the noise strengths from top to below: $D = 0, D = 0.01, D = 0.05, D = 0.1$ ($I = 0, v = 7\text{m/s}, b = 0.2, \tau = 1.25, \alpha = 0.85, \gamma = 1, r = 0.5$)

When "Butterworth lowpass filter of order 5" is applied to the simulated BOLD signalling, then the u_i time series look like as in the following figures.

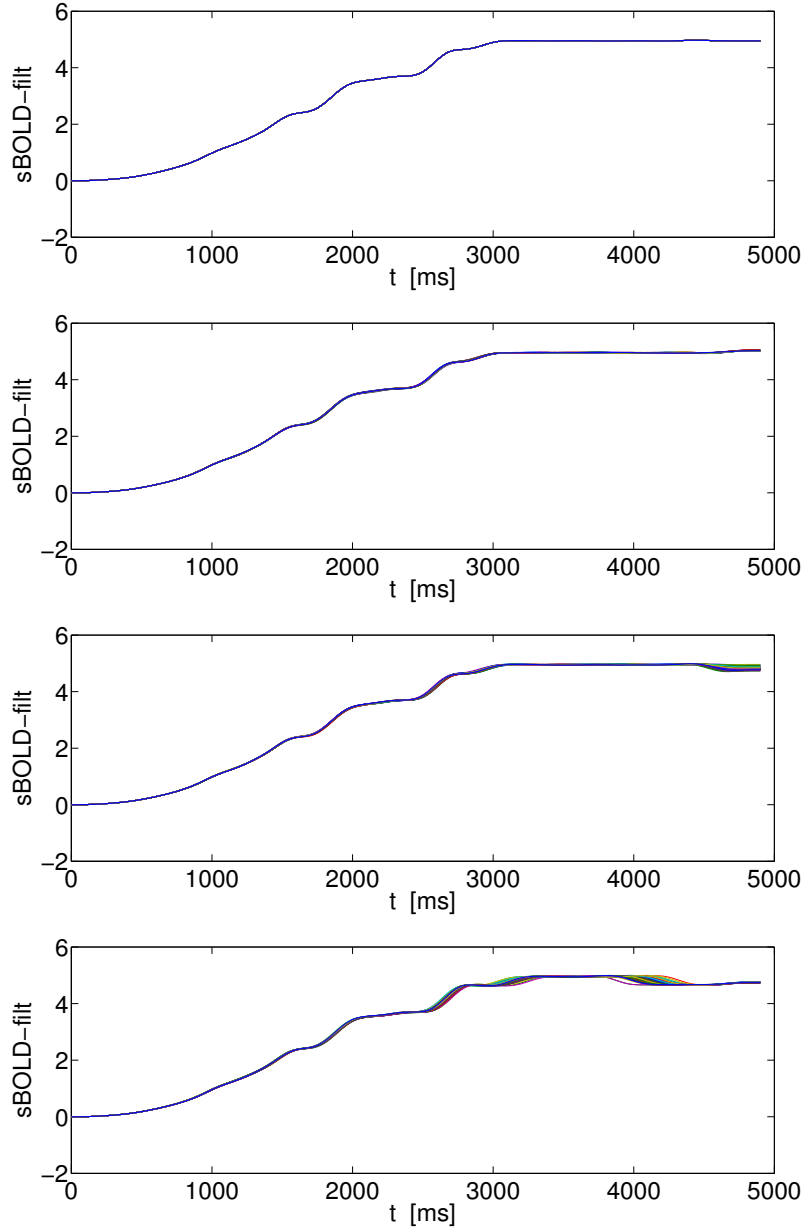


Figure 28, Time evolution of simulated and filtered u_i when $c = 0$, the noise strengths from top to below: $D = 0, D = 0.01, D = 0.05, D = 0.1$ ($I = 0, v = 7m/s, b = 0.2, \tau = 1.25, \alpha = 0.85, \gamma = 1, r = 0.5$)